Article citation info:
ZĘBALA W, SŁODKI B, STRUZIKIEWICZ G. Productivity and reliability improvement in turning Inconel 718 alloy – case study. Eksploatacja i Niezawodnosc – Maintenance and Reliability 2013; 15 (4): 421–426.

Wojciech ZĘBALA
Bogdan SŁODKI
Grzegorz STRUZIKIEWICZ

PRODUCTIVITY AND RELIABILITY IMPROVEMENT IN TURNING INCONEL 718 ALLOY – CASE STUDY

POPRAWA PRODUKTYWNOŚCI I NIEZAWODNOŚCI TOCZENIA STOPU INCONEL 718 – STUDIUM PRZYPADKU*

The paper presents an investigation of Inconel 718 alloy finishing turning, using a procedure that allows the optimal cutting data to be found with a maximization of the metal removal rate as the optimization criterion. The optimization procedure does not allow the required values of the chosen surface roughness indicator, cutting force and cutting tool wedge temperature to be exceeded at the same time. The optimization procedure includes the preliminary cutting tests for establishing the range of cutting data (feed and depth of cut) for the correct chip breaking as well as research concerning micro-hardness measurements which enables the cold work zone to be determined and the minimal value of the feed to be defined. The functionality of the algorithm was verified by using the improvement in machining productivity and reliability of an aircraft engine element as an example.

Keywords: Inconel, turning, productivity, optimization, parameters, micro-hardness.

Artykuł opisuje badania obróbki wykończeniowej toczeniem stopu Inconel 718, mające na celu optymalizację parametrów skrawania z uwzględnieniem maksymalizacji objętościowej wydajności obróbki, jako kryterium optymalizacyjnego. Proponowana procedura uwzględnia wymagane w procesie ograniczenia dotyczące wartości parametru chropowatości obrabianej powierzchni, siły skrawania oraz maksymalnej temperatury w strefie skrawania. Procedura optymalizacyjna zawiera wstępne testy mające na celu ustalenie w lokalnych warunkach obróbki użytecznego zakresu parametrów skrawania (posuwu i głębokości skrawania) dla otrzymania korzystnej postaci wiórów. Wykonane pomiary mikrotwardości w strefie skrawania umożliwiły określenie wielkości strefy zgniotu warstwy wierzchniej, co z kolei pozwoliło na zdefiniowanie minimalnej wartości posuwu. Procedurę optymalizacyjną zweryfikowano na przykładzie obróbki wybranej powierzchni elementu silnika lotniczego. Osiągnięto znaczną poprawę produktywności i niezawodności procesu obróbki.

Słowa kluczowe: Inconel, toczenie, produktywność, optymalizacja, parametry, mikro-twardość.

Nomenclature

A_D	cutting layer cross section in mm^2
a_p	depth of cut in mm
D_c	work piece diameter in mm
f	feed rate in mm/rev
F_c F_f F_p	components of cutting force in N
i	number of passes
n	rotational speed in rev
Q_v	metal removal rate in cm^3/min
Ra	surface roughness in µm
t_1	cutting time for one pass in min
T_{cut}	temperature in °C
t_{cut}	total time of cutting in min
v_c	cutting speed in m/min
R^2	coefficient of determination

1. Introduction

Nickel-based alloys (HRSA) due to their good mechanical properties in high temperatures are commonly used in the aerospace industry, e.g. for parts in gas turbine engines. The most popular types of HRSA include Inconel 718, Inconel 625 and Waspaloy. About 45% of forgings and 15% of casts are made of Inconel 718 alloy [6, 29].

Although nickel-based alloys have good constructional properties they are difficult-to-cut materials. Inconel 718 can be characterized by high hardness and high strength in elevated temperature which leads to high cutting resistance. This alloy has a tendency to work surface hardening. Its low thermal conductivity leads to high temperature developing in the cutting zone. These rise from around 900 °C at a low cutting speed of 30 m/min up to 1300 °C at 300 m/min [18].

Most nickel-based alloys' chemical composition includes 10–20% chromium, up to 8% aluminium and titanium combined, from 5 to 15% cobalt and small quantities of boron, zirconium, magnesium and carbon. The other additives include molybdenum, niobium and tungsten.

From the end of the seventies nickel alloys were the object of detailed research [4, 10, 12, 13, 15, 21–23, 26, 27, 34]. A lot of attention was paid to the quality of the surface and the integrity of the upper layer of elements made of nickel-based alloys [24, 31]. This is important for the durability, endurance fatigue, productivity and functionality of machined parts [2, 3, 5, 35, 36].

The machining process can take place only when the necessary force, properly situated in space and time, is applied to the work piece. The force acting on the cutting wedge must overcome the resistance of the work piece material, its elastic and plastic strains, and frictional resistance when a new surface is created [9, 28, 33].

An analysis of the bibliography, describing the phenomena taking place in the machining process, reveals the fact that when the cutting speed increases (with a constant value for the metal removal rate) the

(*) Tekst artykułu w polskiej wersji językowej dostępny w elektronicznym wydaniu kwartalnika na stronie ***www.ein.org.pl***

cutting force decreases [14]. This enables thin-walled work pieces to be machined.

The influence of the cutting speed on the cutting force and the surface roughness is connected with the influence of the deformation speed of the cutting layer on the plasticity of the machined material and tool wear [11, 16]. The temperature in the cutting zone is closely related to the cutting speed and in general increases when the cutting speed increases. Heat changes the alloy microstructure and causes stress formation [25]. When a low cutting speed is applied, abrasive wear on the tool flank face is dominant [8]. A higher cutting speed causes adhesion wear and high cutting speed is also connected with diffusion wear [20].

There are many papers devoted to the optimization of Inconel 718 machining. The problems concerning the cutting optimization of Inconel 718 alloy, together with the optimization criterion of the surface roughness was presented in [1, 16–18, 35]. In [1] the optimization of the hybrid machining process with economical criterion was analysed. Another approach to machining data optimization was presented in [7], the main criterion being the maximization of tool life and the minimization of production cost.

A similar approach concerning the optimization of milling cutting data was presented by the authors in [19]. The optimization of cutting data by means of RSM (Response Surface Methodology) for ceramic tools was considered in [1]. A genetic algorithm coupled with an artificial neural network (ANN) as an intelligent optimization technique for machining parameters optimization of Inconel 718 was described in [30]. On the other hand, HSC turning optimization by means of Taguchi Grey Relational Analysis was described in [26].

Due to the physical properties of Inconel 718, as well as work piece surface hardening as a result of surface deformation and low thermal conductivity, there is a lack of specific results for machining process optimization with a productivity criterion. Thus, the authors tried to determine a procedure to find the optimal cutting data for Inconel 718 alloy finishing turning with a maximization of the metal removal rate (productivity) as the optimization criterion, that at the same time did not exceed the required values of the surface roughness indicators, cutting force and tool wedge temperature. The verification of the correctness of the algorithm's working is described in section 3.

2. Optimization procedure

The problem of a turning improvement with the optimization criterion of the maximum metal removal rate can be formulated in the following way, Eqs. (1–7):

$$a_{p\,min} \le a_p \le a_{p\,max} \quad (1)$$

$$f_{min} \le f \le f_{max} \quad (2)$$

$$v_{c\,min} \le v_c = f(n, D_c) \le v_{c\,max} \quad (3)$$

$$Q_v = f(v_c, f, a_p) \rightarrow Q_{v\,max} \quad (4)$$

$$F \le F_{lim} \quad (5)$$

$$T_{cut} \le T_{cut\,lim} \quad (6)$$

$$Ra \le Ra_{\,lim} \quad (7)$$

Where: $Q_{v\,max}$ – maximum metal removal rate; $Ra_{\,lim}$ – required value of surface roughness; F_{lim} – acceptable value of cutting force components ($F_{c\,lim}$, $F_{f\,lim}$, $F_{p\,lim}$), due to the strength of the grip part and the direct influence of the work piece surface layer properties; $T_{cut\,\,lim}$ – acceptable temperature limit of the tool wedge.

Eqs. (1–3) determine the collection of the allowable values of the depth of cut, feed and cutting speed. The ranges for these values are based on the tool manufacturer's recommendations and specific investigations in the local machining conditions (e.g. correct chip breaking). The general productivity improvement procedure, based on experiments, is presented in Fig. 1. At the beginning of the procedure a range of cutting data and process optimization criterion must be defined. On the basis of the results, obtained from the successive steps of the optimization process, the correct cutting data can be selected. The scheme presented in Fig. 1 consists of the following steps:

(1) Definition of optimization criterion (Q_v in this approach) and optimization limits (F, T_{cut} , Ra).
(2) Preliminary cutting tests for establishing the cutting data range for correct chip breaking.
(3) Establishment of the research method and measurement equipment. At this stage it is necessary to determine the final cutting data range for the tests.
(4) Measurement tests (F, Ra, T_{cut}) for selected cutting data.
(5) Research concerning micro-hardness measurements, which enables the reach of the cold work zone to be determined.
(6) Determination and analysis of $F = f(Q_v)$, $T_{cut} = f(Q_v)$ and $Ra = f(Q_v)$ functions.
(7) Analysis of the above functions leads to setting the optimal cutting data that fulfils the optimization criterion and limits.

3. Verification of the optimization procedure

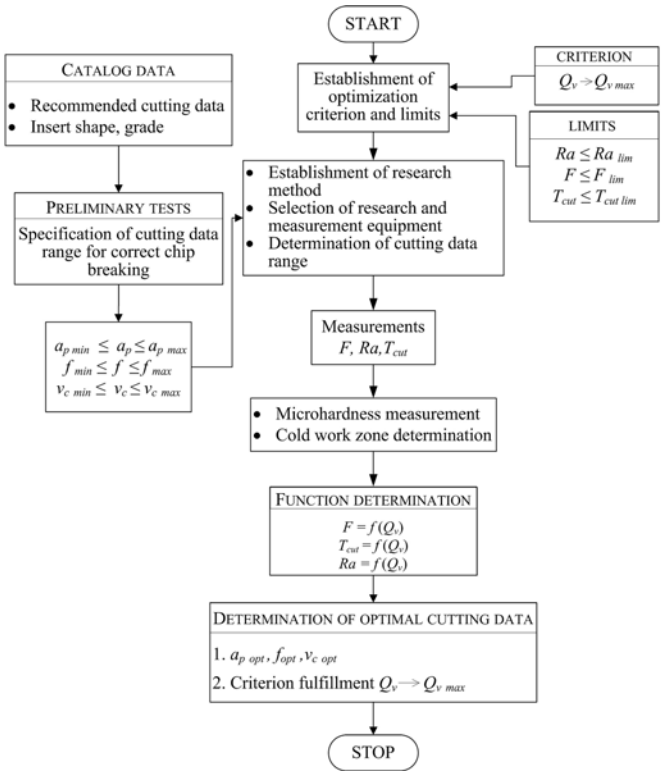

Fig. 1. Scheme of the productivity improvement procedure during turning ($Q_{v\,max}$)

The optimization process of cutting data selection, according to the outline presented in Fig. 1, was performed for the selected surface (**) of the aircraft engine element (bush), manufactured using Inconel 718 alloy, Fig. 2a. The initial cutting data (Case1), selected from the tool manufacturer's recommendations (a_p, f and v_c) and the calculated values are shown in Table 1.

The surface roughness measured from the data was $Ra = 0.95$ µm at $Q_v = 3{,}52$ mm^3/min. These were initial cutting data with reference

Table 1. Initial cutting data and calculated values A_D, t_1 and t_{cut}

	a_p mm	f mm/rev	v_c m/min	A_D mm^2	t_1 min	t_{cut} min	i
Case1	1.1	0.080	40	0.088	0.374	2.25	6

to which the optimal parameters were investigated. Cutting experiments were performed on the research stand built on the base of the turning centre, with the cutting force measurement device. Fig. 2b is a photograph taken during the external surface machining of the element shown in Fig. 2a.

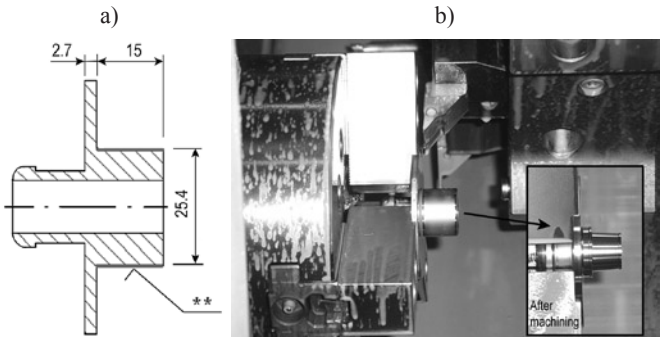

Fig. 2. Shape of semi-finished product (a) and photo of its machining (b)

Turning was carried out with a sintered carbide insert, VCMT 160404-SM with TiAlN coating, and $\alpha_n = 7^o$ clearance angle. The cutting insert was mounted in the tool-holder, SVJCR 2020K-16.

The optimization criterion – (maximization of Q_v) and constraints, Eq. (8) were determined as the first step of the procedure. F_f feed force and F_p radial force were not considered.

$$Ra \leq 1{,}15\ \mu\text{m and } F_c \leq 470\ \text{N and } T_{cut} \leq 650\ ^{o}\text{C} \qquad (8)$$

An analysis of SM type chipbreaker efficiency in an actual, local machining environment was performed and described in details [32, 37]. The results for $v_c = 50$ m/min are presented in Fig. 3a. The marks in this figure mean: "×" – unacceptable chip form, "0" – acceptable chip form, "+" – correct chip form. The main dimensions of the rake face shape are shown at the top. The conveyed tests revealed the fact that the most profitable chip forms came into being within the following range: cutting speed $v_c = 40$-60 m/min, feed $f = 0.08$-0.25 mm/rev and depth of cut $a_p > 1$ mm.

The values obtained for F_c cutting force and T_{cut} temperature, as a function of the feed and cutting speed, are presented in Fig. 3b and Fig. 4a, respectively. Examples of thermograms for the highest and the lowest temperature in the cutting zone, measured by means of an infrared camera, are shown in Fig. 4b and Fig. 4c, respectively.

When considering Fig. 3b it can be observed that for feed values greater than 0.1 mm/rev the cutting force increases more slowly as the feed increases. Generally, when the feed rises, the cross section of the cutting layer enlarges and the cutting resistance increases. With a feed value over 0.1 mm/rev only a slight increase in the cutting force occurs. This is due to the fact that a material decohesion process takes place below the cold work layer and the cutting resistance decreases. This is confirmed by the micro-hardness measurements of the work material in the cutting zone, described below. It suggests establishing a higher feed limit (over 0.1 mm/rev) than was initially proposed (0.08 mm/rev).

The influence of the cutting speed on the cutting wedge temperature is shown in Fig. 4. At a greater cutting speed, the temperature of the work material in the cutting zone is higher, which decreases the strength of the material being cut.

Observing the cutting wedge temperatures for different feed and cutting speed values it can be stated that as the feed increases up to about 0.18 mm/rev a decrease in temperature occurs. This probably is directly linked to the decrease in the thickness of the cold work layer in relation to the total thickness of the cutting layer. The cutting wedge temperature reaches a minimum value for each cutting speed in the

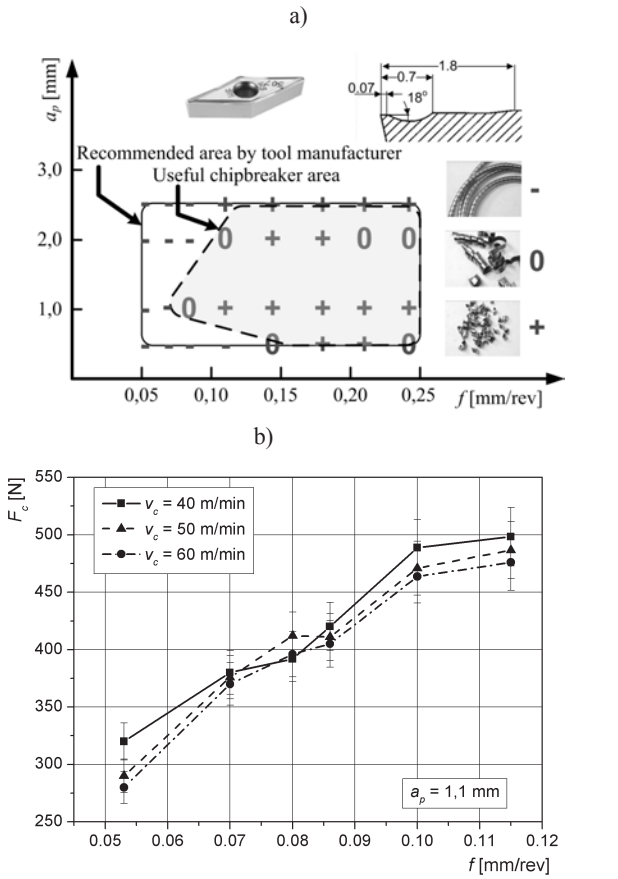

Fig. 3. Classification of chips forms with useful chipbreaker area type SM in local testing environment for v_c=50 m/min, (a) and influence of feed on cutting force (b)

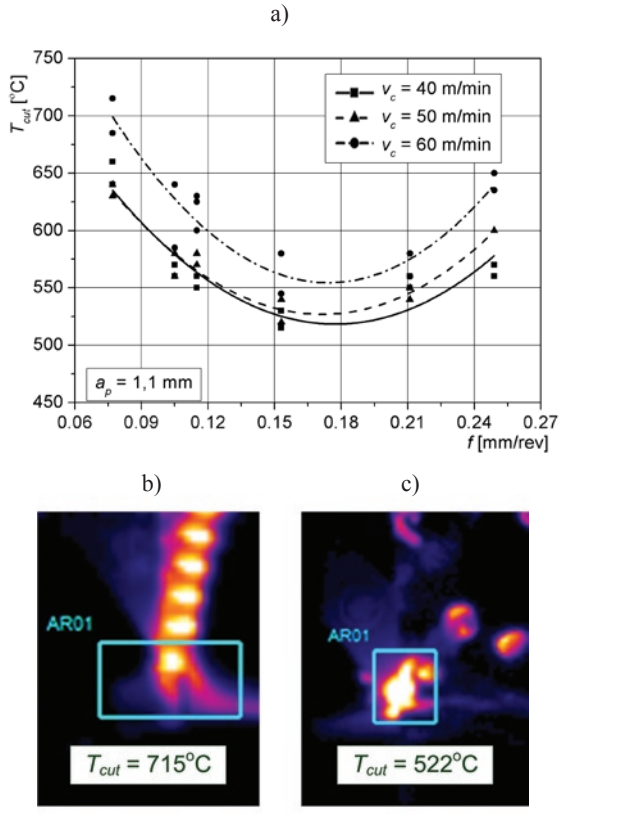

Fig. 4. Temperature of tool wedge: a) $T_{cut} = f(f, v_c)$, b) infra-red photo for v_c=60 m/min and f =0.08 mm/rev, c) infra-red photo for v_c=40 m/min and f =0.15 mm/rev

region of $f = 0.18$ mm/rev. With a greater feed value the cutting wedge temperature increases as the feed increases on account of the cutting layer cross section increase and simultaneously there is less and less influence from the cold work layer on the decohesion process.

To analyse chip morphology and the cold work zone of machined material, tests in which there was a sudden halt in the cutting process were performed. An example of a micro-section photograph, taken by a scanning microscope, is presented in Fig. 5a. The austenitic structure of the material, the size of the grain and the location of the infrequent titanium carbide particles can be observed (arrows in the picture).

Next, the micro-hardness $HV_{0.1}$ (Hannemann method) in the cutting zone, along the line situated inside the chip and the work piece (line AB in Fig. 5a), was measured. The diagram illustrating the influence of the cutting speed on the micro-hardness distribution for a feed $f = 0.1$ mm is presented in Fig. 5b.

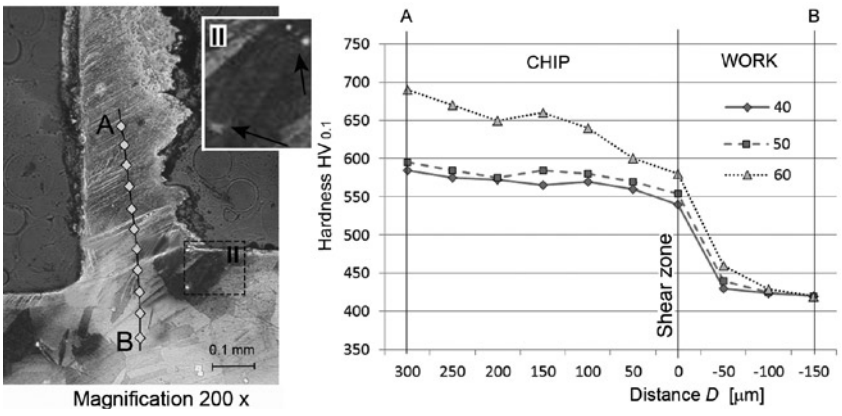

Fig. 5. Chip creation zone with titanium carbide particles indicated by arrows (a) and micro-hardness distribution along AB line for the feed $f = 0.1$ mm and cutting speed v_c = 40;50;60 m/min (b)

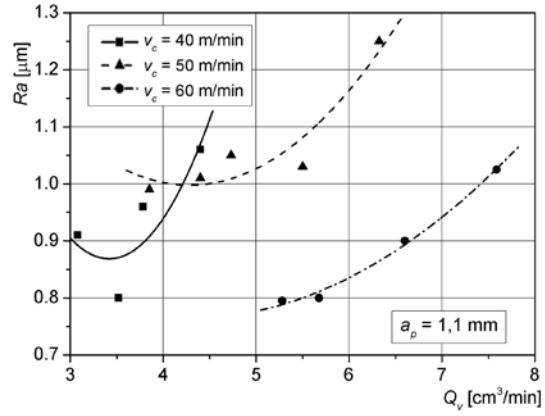

Fig. 6. Dependence of roughness parameter of machined surface Ra from metal removal rate for different cutting speeds

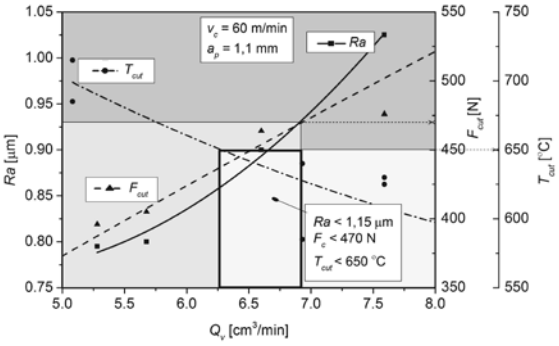

Fig. 7. Dependence of F_c, T_{cut} and Ra from metal removal rate for v_c = 60 m/min

Nickel based alloys harden during machining, which is caused by a significant plastic deformation in the area located straight in front of the cutting wedge. The size of this deformation changes as a function of the distance from the machined surface. It translates into a hardness increase from 420 $HV_{0.1}$ for the core material (near point B), to 540;554;580 $HV_{0.1}$ in the shear zone for v_c = 40;50;60 m/min, respectively, Fig. 5b. At a distance of approximately 0.1 mm from the machined surface, a significant decrease in hardness can be observed of 425–429 $HV_{0.1}$. This means that a feed of at least 0.1 mm or above should be recommended, so as to move the cutting edge below a hardened layer of the material. The results of the roughness measurements of the machined surface for different metal removal rates are presented in Fig. 6.

It can be observed, that at a slower cutting speed the roughness parameter *Ra* reaches acceptable values below 0.95 μm but the metal removal rate is low, below 4 cm³/min. So, it seems to be reasonable to apply a cutting speed over 50 m/min.

Taking into consideration the investigations described above, appropriate ranges for the feed (0.1 mm $\leq f \leq$ 0.25 mm) and cutting speed (50 m/min $\leq v_c \leq$ 60 m/min) values were established. The depth of cut was set as in Case 1.

Using the measured data and the calculations, the diagram in Fig. 7 was created. The diagram enables the best values for the cutting data, which fulfil the imposed optimization limitations (8), to be selected.

The diagram in Fig. 7 with the Eqs. (9-11) permits the maximum metal removal rate for the cutting speed v_c = 60 m/min to be determined. This value was chosen from a range fulfilling the limit of T_{cut} temperature (diagram in Fig. 4a).

$$Ra = 1.20005 - 0.20395Q_v + 0.02386Q_v^2 \quad (R^2 = 0{,}98162) \quad (9)$$

$$T_{cut} = 1018.31177 - 80.68902Q_v + 3.50898\,Q_v^2 \quad (R^2 = 0{,}97467) \quad (10)$$

$$F_c = 96.5146 + 58.97511Q_v - 0.73246\,Q_v^2 \quad (R^2 = 0{,}97987) \quad (11)$$

The optimized cutting data were chosen for the maximum metal removal rate $Q_v = 6.92$ cm³/min and these are presented in Table 2.

Table 2. Previously applied (Case1) and optimized cutting data for v_c = 60 m/min

	a_p mm	f mm/rev	v_c m/min	Ra μm	Q_v cm³/min	T_{cut} °C	F_c N
Initial cutting data (Case1)	1.1	0.080	40	0.95	3.52	580	392
Optimized cutting data	1.1	0.105	60	0.93	6.92	628	469

4. Conclusion

The results of the experimental tests allowed the best values for the cutting data in the conditions determined for the bush external surface machining, made of Inconel 718, to be established due to the maximization of the metal removal rate at the set limit values of F_c, T_{cut} and *Ra*. As a result of the optimization procedure an almost 97% productivity increase was achieved at, with a simultaneous small-scale

increase of surface roughness, up to the parameter value Ra = 1,1 μm (admissible value Ra_{lim} = 1,15 μm) and an increase in the cutting force value by about 20% to the admissible limit. The machining process is more reliable taking into account the good chip formation and breaking for the optimized cutting data. The research proved the necessity for preliminary live machining tests in local operating features, which serve as a source of information for the optimization procedure.

References

1. Aruna M, Dhanalaksmi V. Design optimization of cutting parameters when turning Inconel 718 with cermet inserts. World Academy of Science, Engineering and Technology 2012; 61:952–956.
2. Arunachalam RM, Mannan MA, Spowage AC. Residual stress and surface roughness when facing age hardened Inconel 718 with CBN and ceramic cutting tools. International Journal of Machine Tools and Manufacture 2004; 44:879–887.
3. Arunachalam RM, Mannan MA, Spowage AC. Surface integrity when machining age hardened Inconel 718 with coated carbide cutting tools. International Journal of Machine Tools and Manufacture 2004; 44:1481–1491.
4. Arunachalam RM, Mannan MA. Machinability of nickel-based high temperature alloys. Machining Science and Technology 2000; 4:127–168.
5. Axinte DA, Gindy N, Fox K, Unanue I. Process monitoring to assist the workpiece surface quality in machining. Machine Tools and Manufacture 2004; 44:1091–1108.
6. Choudhoury IA, El-Baradic MA. Machinability of nickel-base super alloys: a general review. Materials Processing Technology 1998; 77:278–284.
7. Choudhoury SK, Appa Rao IVK. Optimization of cutting parameters for maximizing tool life. International Journal of Machine Tools & Manufacture 1999; 39:343–353.
8. D'Addona D, Segreto T, Simeone A, Teti R. ANN tool wear modelling in the machining of nickel superalloy industrial products. CIRP Journal of Manufacturing Science and Technology 2011; 4:33–37.
9. Devillez A, Schneider F, Dominiak S, Dudzinski D, Larrouquere D. Cutting forces and wear in dry machining of Inconel 718 with coated carbide tools. Wear 2007; 262:931–942.
10. Dudzinski D, Devilleza A, Moufkia A, Larrouquèreb D, Zerroukib V, Vigneaub J. A review of developments towards dry and high speed machining of Inconel 718 alloy. International Journal of Machine Tools and Manufacture 2004; 44:439–456.
11. El-Hossainy TM, El-Zoghby AA, Badr MA, Maalawi KY, Nasr MF. Cutting Parameter Optimization when Machining Different Materials. Materials and Manufacturing Processes 2010; 25:1101–1114.
12. Ezugwu EO, Fadarea DA, Bonneya J, Da Silvaa RB, Salesa WF. Modelling the correlation between cutting and process parameters in high-speed machining of Inconel 718 alloy using an artificial neural network. International Journal of Machine Tools & Manufacture 2005; 45:1375–1385.
13. Ezugwu EO. Key improvements in the machining of difficult-to-cut aerospace superalloys. International Journal of Machine Tools and Manufacture 2005; 45:1353–1367.
14. Fang N, Wu Q. A comparative study of the cutting forces in high speed machining of Ti–6Al–4V and Inconel 718 with a round cutting edge tool. Journal of Materials Processing Technology 2009; 209:4385–4389.
15. Gullu A, Karabulut S. Dynamic Chip Breaker Design for Inconel 718 Using Positive Angle Tool Holder. Materials and Manufacturing Processes 2008; 23:852–857.
16. Guo YB, Li W, Jawahir IS. Surface Integrity Characterization and Prediction in Machining of Hardened and Difficult-To-Machine Alloys: A State-Of-Art Research Review and Analysis. Machining Science and Technology 2009; 13:437-470.
17. Jonak J, Podgórski J, Zubrzycki J. Wybrane zagadnienia mechaniki procesu skrawania materiałów. Eksploatacja i Niezawodnosc – Maintenance and Reliability 2001; 5:27–31.
18. Kitagawa T, Kubo A, Maekawa K. Temperature and wear of cutting tools in high-speed machining of Inconel 718 and Ti-6Al-6V-2Sn. Wear 1997; 202:142–148.
19. Krain HR, Sharman ARC, Ridgway K. Optimization of tool life and productivity when end milling Inconel 718. Materials Processing Technology 2007; 189:153–161.
20. Liao YS, Shiue RH. Carbide tool wear mechanism in turning of Inconel 718 superalloy. Wear. 1996; 193:16–24.
21. Nalbant M, Altin A, Gokkaya H. The effect of cutting speed and cutting tool geometry on machinability properties of nickel-base Inconel 718 super alloys. Materials&Design 2007; 28:1334–1338.
22. Narutaki N, Yamane Y. Machining of difficult-to-cut materials. International Journal of the Japan Society for Precision Engineering 1993; 27:307–310.
23. Narutaki N, Yamanea Y, Hayashib K, Kitagawac T, Uehara K. High-speed machining of Inconel 718 with ceramic tools. CIRP Annals – Manufacturing Technology 1993; 42:103–106.
24. Oktem H, Erzurumlu T, Kurtaran H. Application of response surface methodology in the optimization of cutting conditions for surface roughness. Journal of Materials Processing Technology 2005; 170:11–16.
25. Outeiro JC, Pina JC, M'Saoubi R, Pusavec F, Jawahir IS. Analysis of residual stresses induced by dry turning of difficult-to-machine materials. CIRP Annals – Manufacturing Technology 2008; 57:77–80.
26. Pawade RS, Joshi S. Mechanism of chip formation in high-speed turning of Inconel 718. Machining Science and Technology 2011; 15:132–152.
27. Pawade RS, Joshi S. Multi-objective optimization of surface roughness and cutting forces in high-speed turning of Inconel 718 using Taguchi grey relational analysis (TGRA). The International Journal of Advanced Manufacturing Technology 2011; 56:47–62.
28. Rusinek R. Drgania w procesie skrawania stopu tytanu. Eksploatacja i Niezawodnosc – Maintenance and Reliability 2010; 3:48–55.
29. Sandvik Coromant, Aerospace Engine – application guide 2004.
30. Senthilkumaar JS, Selvarani P, Arunachalam RM. Intelligent optimization and selection of machining parameters in finish turning and facing of Inconel 718. The International Journal of Advanced Manufacturing Technology 2012; 58:885–894.

31. Sharman ARC, Hughes JI, Ridgway K. An analysis of the residual stresses generated in Inconel 718TM when turning. Journal of Materials Processing Technology 2006; 173:359–367.
32. Słodki B, Zębala W. The analysis of selected chipbreakers efficiency in difficult-to-cut material turning in local operating features. Naukowyj Żurnal, National University in Chmielnicki, Ukraine 2007; 1:179–189.
33. Taranenko G, Taranenko W, Świć A, Szabelski J. Modelowanie układów dynamicznych obróbki skrawaniem wałów o małej sztywności. Eksploatacja i Niezawodnosc – Maintenance and Reliability 2010; 4:4–15.
34. Thakur DG, Ramamoorthy B, Vijayaraghavan L. A Study on the Parameters in High-Speed Turning of Superalloy Inconel 718. Materials and Manufacturing Processes 2009; 24:497–503.
35. Wrigth PK, Chow JG. Deformation characteristic of nickel alloys during machining. Journal of Engineering Materials and Technology 1982; 104:85–93.
36. Yoo JT, Yoon JH, Lee HS, Youn SK. Material characterization of Inconel 718 from free bulging test at high temperature. Journal of Mechanical Science and Technology 2012; 26:2101–2105.
37. Zębala W, Słodki B. Some aspects of chipbreakers efficiency in difficult-to-cut materials turning. Proc. of Int. Users' Conf. „Modelling Technology – Machining Solution", Minneapolis, MN, USA 2008; 14:1-14.

Wojciech ZĘBALA, Ph.D., D.Sc. (Eng.)
Bogdan SŁODKI, Ph.D. (Eng.)
Grzegorz STRUZIKIEWICZ, Ph.D. (Eng.)
Production Engineering Institute, Mechanical Faculty
Cracow University of Technology
Al. Jana Pawła II 37, 31-864 Kraków, Poland
E-mail: zebala@mech.pk.edu.pl